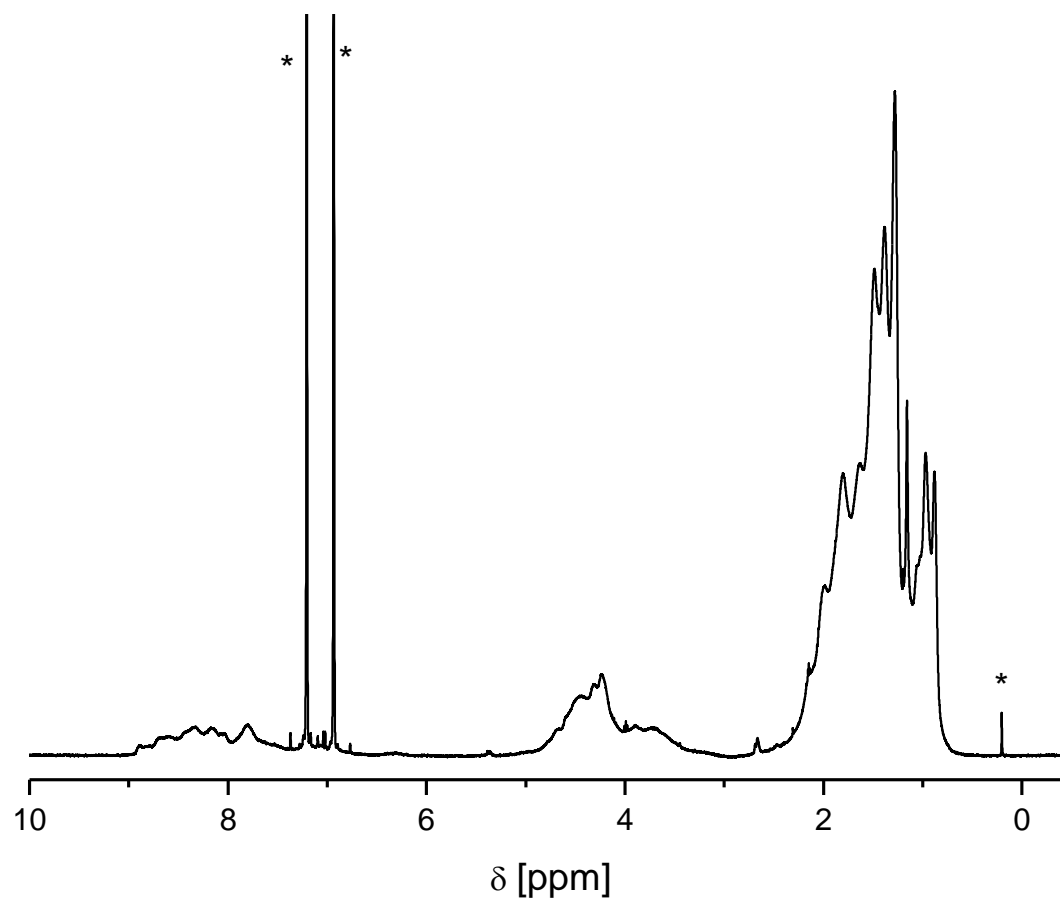
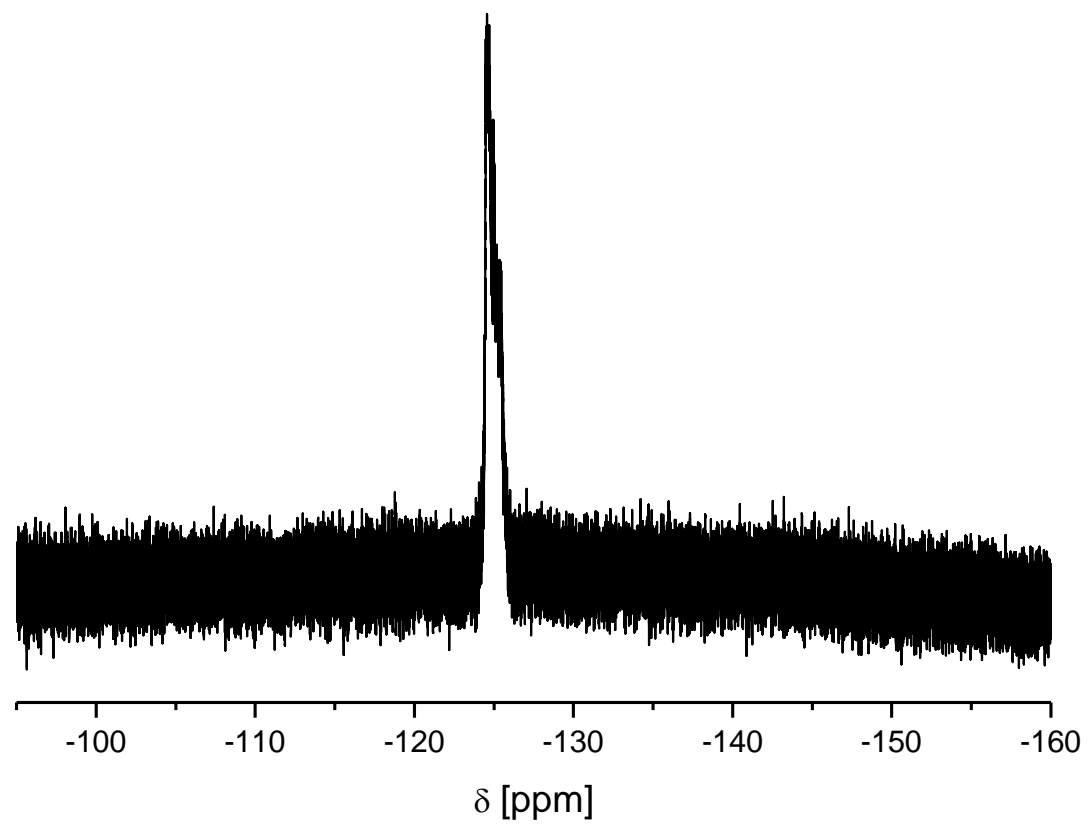


## Electronic supplementary information



**Figure 11.**  $^1\text{H}$  NMR of P4 in 1,2-dichlorobenzene- $\text{d}_4$  at 373 K.



**Figure 2.**  $^{19}\text{F}$  NMR of P4 in 1,2-dichlorobenzene- $\text{d}_4$  at 373 K.

## CV measurements

The cyclic voltammetry (CV) measurements of P4 were carried out applying a computer-controlled VA-Standard 663 and a  $\mu$ Autolab Type III potentiostat of Metrohm AG Suisse. The measurements were performed in dried and oxygen-free acetonitrile using 0.1 M tetrabutylammonium hexafluorophosphate (electrochemical grade, FLUKA) as a supporting electrolyte. A thin polymer film dropcast from chloroform solution on a platinum disk was used as a working electrode, a glassy carbon as a counter electrode and Ag/AgCl as a reference electrode as reported before.<sup>1</sup> Redox potentials were referenced against ferrocene/ferrocenium (Fc/Fc<sup>+</sup>). The corresponding highest occupied molecular orbital (HOMO) and lowest occupied molecular orbital (LUMO) were calculated using the onset of  $E_{ox}$  and  $E_{red}$  and using the absolute value of -4.8 eV to vacuum for the Fc/Fc<sup>+</sup> redox potential. The energy difference between the HOMO and LUMO levels of the polymer measured by CV is the electrochemical band gap ( $E_g^{ec}$ ).

The HOMO and LUMO energy levels of P4 were determined from the oxidation and reduction peaks of the cyclic voltammogram shown in Figure 3. The HOMO and LUMO levels of P4 lay at -5.19 eV and -3.30 eV, respectively. Thus the electrochemical band gap ( $E_g^{ec}$ ) of P4 is 1.89 eV, which is remarkably smaller than those of P2 (2.47 eV) and P3 (2.40 eV) and slightly smaller than that of P1 (2.03 eV), which performed best as a donor polymer in the solar cell experiments of P1 – P3 before.<sup>1</sup>

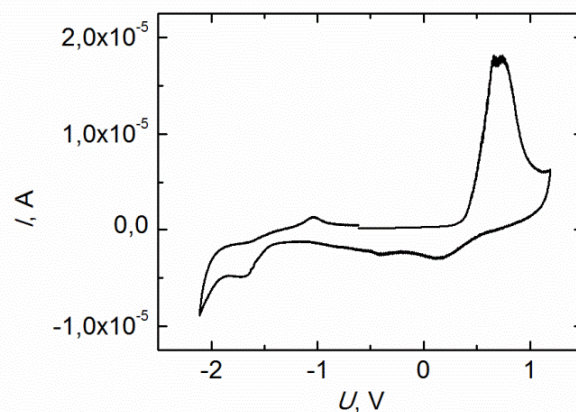


**Figure 3.** The cyclic voltammogram of P4.

### Time correlated single photon counting (TCSPC) measurements

The fluorescence decays of P1 – P3 shown in Figure 4 (left) are clearly one exponential, but that of P4 is two exponential with lifetimes of 0.40 ns and 2.14 ns. Lifetimes and fluorescence decay associated spectra (DAS) for the polymers are displayed in Figure 4 (right). Because the lifetimes of all the polymers are in nanosecond scale and the spectra have relative large Stokes shifts, the polymers are assumed to have different conformations and electron densities in the excited states compared to the ground states in CHCl<sub>3</sub> solution.

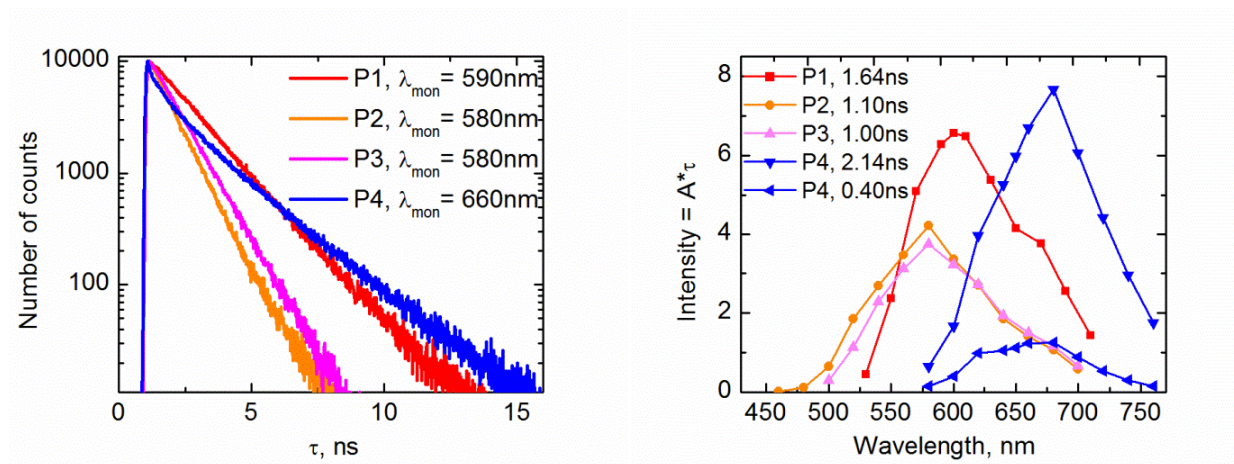


**Figure 4.** Fluorescence decay curves and decay associated spectra (DAS) of P1 – P4 measured in CHCl<sub>3</sub>.

**Table S1** Optical and electrochemical properties of P4.

$\lambda_{\text{abs,max}}$ (eV)	$\lambda_{\text{pL,max}}$ (eV)	$E_g^{\text{opt}*}$ (eV)	HOMO (eV)	LUMO (eV)	$E_g^{\text{ec}}$ (eV)
612	699	1.91	-3.3	-5.19	1.89

\* $E_g^{\text{opt}}$  calculated from the onset values of the absorption spectra in Figure 6.

## DSC measurements

Mettler Toledo DSC821e thermo analyzer was applied for differential scanning calorimetry (DSC) measurements. To compare the thermodynamic stability of polymers P4 and P1, 2 mg samples of the polymers were heated from 25 °C to 500 °C by dynamic 20 °C/min heating rate in a standard 40  $\mu$ L perforated Al crucible with 60 mL/min N<sub>2</sub> flow. To remove the thermal history and to further observe the ongoing thermodynamic processes 4.57 mg of P4 and 4.47 mg of P1 were heated three times from -70 °C to 300 °C and from -70 °C to 400 °C, respectively, with a heating rate of 20 °C/min and cooled back to -70 °C.

Thermal properties of the synthesized P4 were measured by DSC and compared with those of P1 – P3 reported<sup>1</sup> before. P1 was used as reference sample. The heating scans of P1 and P4 from 25 °C to 500 °C are shown in Figure 5, where P1 exhibits a broad exothermic peak around 400 °C and right after that a strong endothermic peak, which are probably due to degradation of the polymer. A strong exothermic rise after 450 °C seems to be caused by the oxidation of P1. The curve of P4 is relatively straight until 350 °C and after that exhibits constant exothermic rise, which could be due to degradation of the polymer. The third heating scans between 0 °C and 300 °C are shown in Figure 6. After removing the thermal history, a small endothermic transition of P1 appeared at 216 °C, which is close to the earlier reported<sup>2</sup> endothermic transition of P1 at 205 °C. P4 did not show any clear thermodynamic transitions between 0 °C and 300 °C. Thus P4 is considered amorphous and thermodynamically more stable than P1 in the measured temperature range.

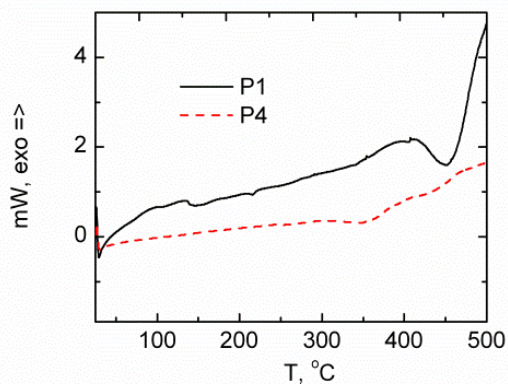


**Figure 5.** The heating scans of P1 and P4 from 25 °C to 500 °C.

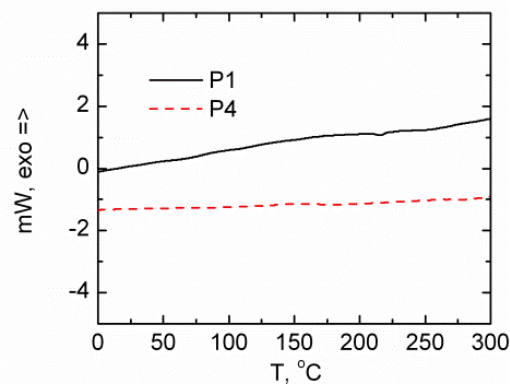


**Figure 6.** The heating scans of P1 and P4 from 0 °C to 300 °C.

1 F. M. Pasker, M. F. G. Klein, M. Sanyal, E. Barrena, U. Lemmer, A. Colsmann and S. Höger, *J. Pol. Sci. A: Pol. Chem.*, 2011, 49, 5001 – 5011.

### Resistances of the cells calculated from the *I-V* curves

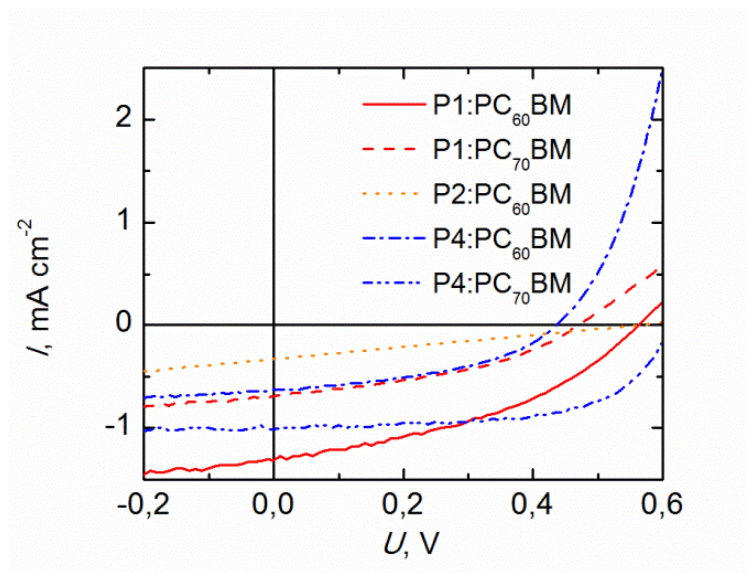


**Figure 7.** *I-V* curves of the aged solar cells with the active layer composition of P1/P2/P4:PC<sub>60</sub>BM/PC<sub>70</sub>BM.

**Table S2** Resistances of the cells calculated based on the IV-curves measured the following day after preparation and after ageing.

Active layer composition	$R_s^a$	$\Omega \text{ cm}^2$	$R_s^b$	$\Omega \text{ cm}^2$	$R_{sh}^a$	$\Omega \text{ cm}^2$	$R_{sh}^b$	$\Omega \text{ cm}^2$
P3HT:PC <sub>60</sub> BM	17.18		54.07		2170		1720	
P1:PC <sub>60</sub> BM	96.06		211.6		1015		1078	
P1:PC <sub>70</sub> BM	173.3		235.5		971.7		1514	
P2:PC <sub>60</sub> BM	319.5		1656		719.9		1688	
P4:PC <sub>60</sub> BM	42.40		78.60		1215		1969	
P4:PC <sub>70</sub> BM	17.42		90.91		2759		7062	

<sup>a</sup>one day after preparation, <sup>b</sup>aged cell

## AFM measurements

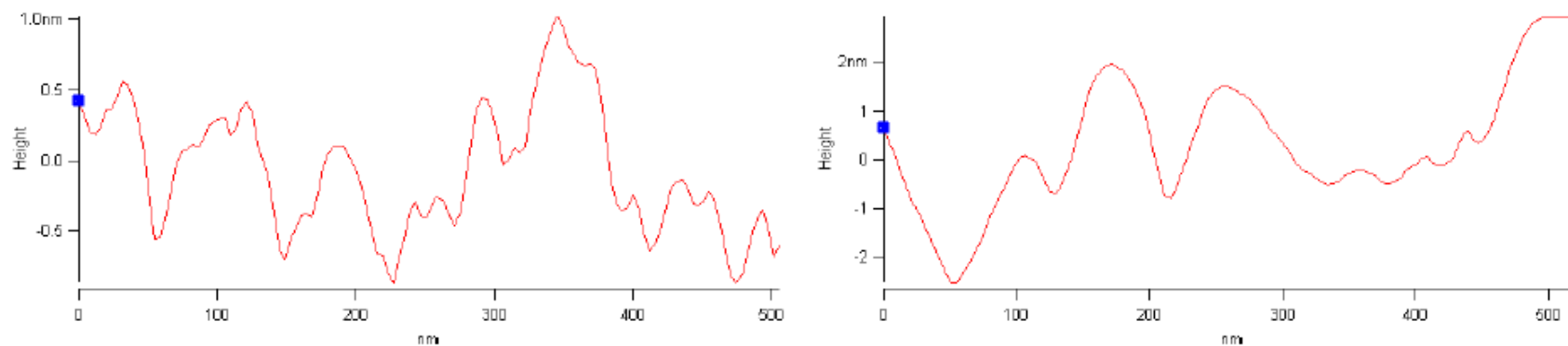


**Figure 8.** Cross section curves of P1:PC<sub>60</sub>BM (left)/PC<sub>70</sub>BM (right) cells.

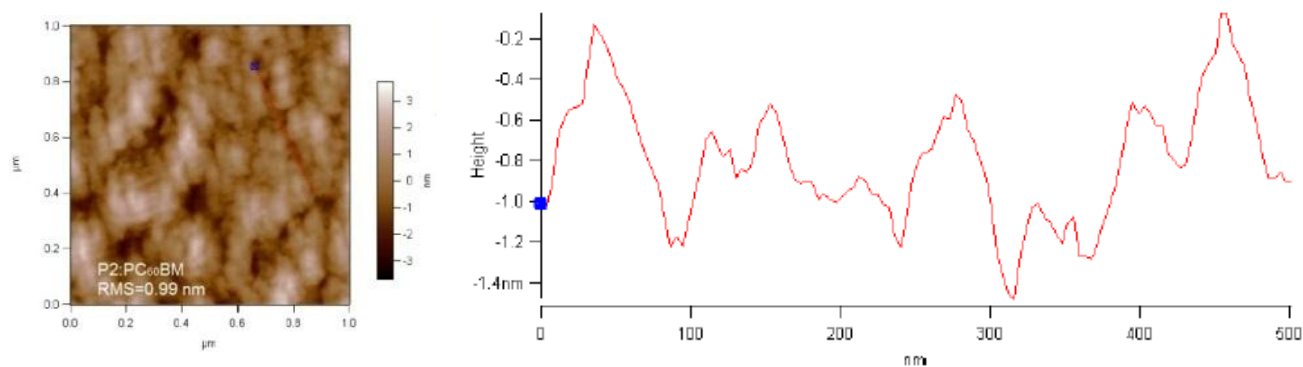


**Figure 9.** AFM image and cross section curve of P2:PC<sub>60</sub>BM cell.

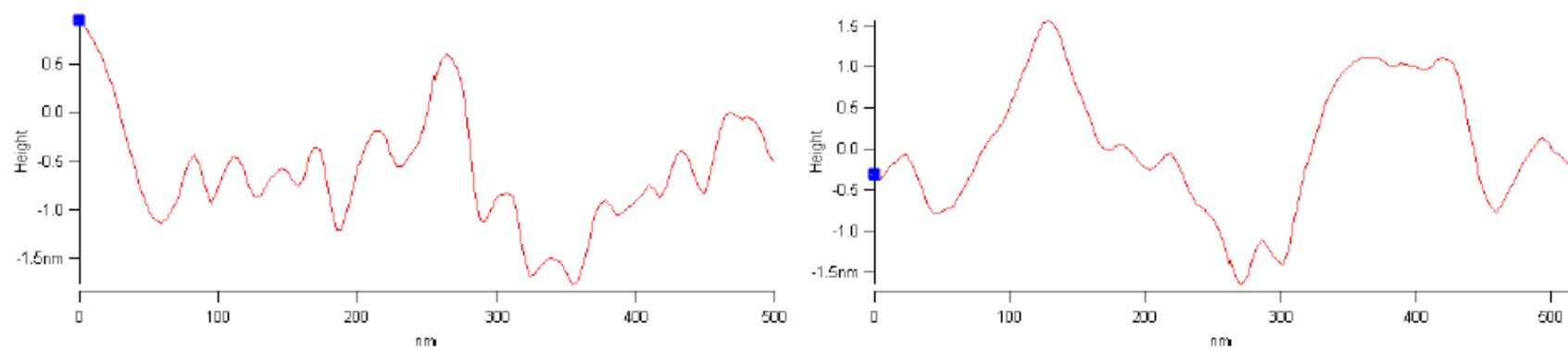


**Figure 10.** Cross section curves of P4:PC<sub>60</sub>BM (left )/PC<sub>70</sub>BM cells (right).

## Computational models

Coordinates of the periodic structures and the longest oligomer models of polymers P1–P4 are given in a zip file **structures.zip**.

## Calculated HOMO-LUMO gaps of oligomers and periodic models

The calculated HOMO-LUMO gaps of oligomer models and HOCO-LUCO gaps of periodic models are given in Table S3.

**Table S3.** Calculated HOMO-LUMO gaps of oligomer models and HOCO-LUCO gaps of periodic models.

	n=1	n=2	n=3	n=4	n=5	n=6	n=7	n=8	periodic
P1	2.73	2.47	2.39	2.35	2.34	2.33	2.32	-	2.30
P2	3.03	2.80	2.74	2.72	2.71	2.70	-	-	2.63
P3	2.96	2.73	2.67	2.64	2.63	2.63	-	-	2.57
P4	3.02	2.49	2.30	2.21	2.16	2.13	2.12	2.10	2.01

## TD-DFT basis set

The basis set used for TD-DFT calculations is rather small (6-31G\*), especially as the oligomers contain sulphur and fluorine. Additional TD-DFT calculations were done using 6-311+G\* basis set for sulphur only, for sulphur and electronegative atoms oxygen and fluorine, and finally, for all atoms. The results were similar with all oligomers P1-P4. We present results for short (n = 1 – 3) P1 oligomers in Table S4.

**Table S4.** TD-DFT excitation energies (eV) for short P1 oligomers

	n=1	n=2	n=3
6-31G*	2.44	2.16	2.07
6-31G*/S:6-311+G*	2.44	2.16	2.07
6-31G*/OFS: 6-311+G*	2.40	2.13	2.04
6-311+G*	2.34	-	-

We note that using 6-311+G\* for only sulphur does not have noticeable effects on excitation energies. When 6-311+G\* is used for O, F and S atoms, the excitation energies are up to 0.04eV smaller than with 6-31G\* basis set. Finally, going for 6-311+G\* basis set on all atoms causes noticeable 0.10 eV

decrease in the monomer excitation energy compared to the 6-31G\* basis set. While the 6-31G\* basis set is small, we are confident that the error caused by it is rather small on long oligomers ( $n=6$ ), most likely smaller than 0.05 eV and similar in all the different (P1–P4) oligomers. Additionally, increasing the basis set did not affect the contributions of the excitations and HOMO→LUMO contribution remains dominant with comparable coefficients as with 6-31G\*.

### **Maximum conducive chain length ( $N_{MCC}$ ):**

To determine the  $N_{MCC}$  values we have plotted the HOMO-LUMO gaps of polymers P1–P4 as a function of  $1/N$  ( $N$  = number of the conjugated double bonds in the polymer backbone). The HOMO-LUMO gap of an infinite polymer and data points of the steepest descending part (also called the linear part) of the curve are needed. The  $1/N_{MCC}$  value is obtained from the intersection of the line  $y(x) = b$  drawn from the HOMO-LUMO gap of an infinite polymer and the line drawn through the steepest descending part of the HOMO-LUMO curve, see Figure 11.

The gap of the infinite polymer can be either calculated using a periodic polymer model or extrapolated from the gaps of the oligomer models. The latter approach was used in this work. The data points of the curve were obtained from the gaps of the oligomer models, as well. If the CRU of the polymer is too large, there are only few data points in the linear part of the curve or the linear part may be even missing or cannot be accurately identified. For the polymers P2 and P3 the linear part cannot be accurately identified, and therefore, the  $N_{MCC}$  values should be considered to be upper limits. The method of determination of the  $N_{MCC}$  values for polymers P1–P4 is illustrated in Figure 11.

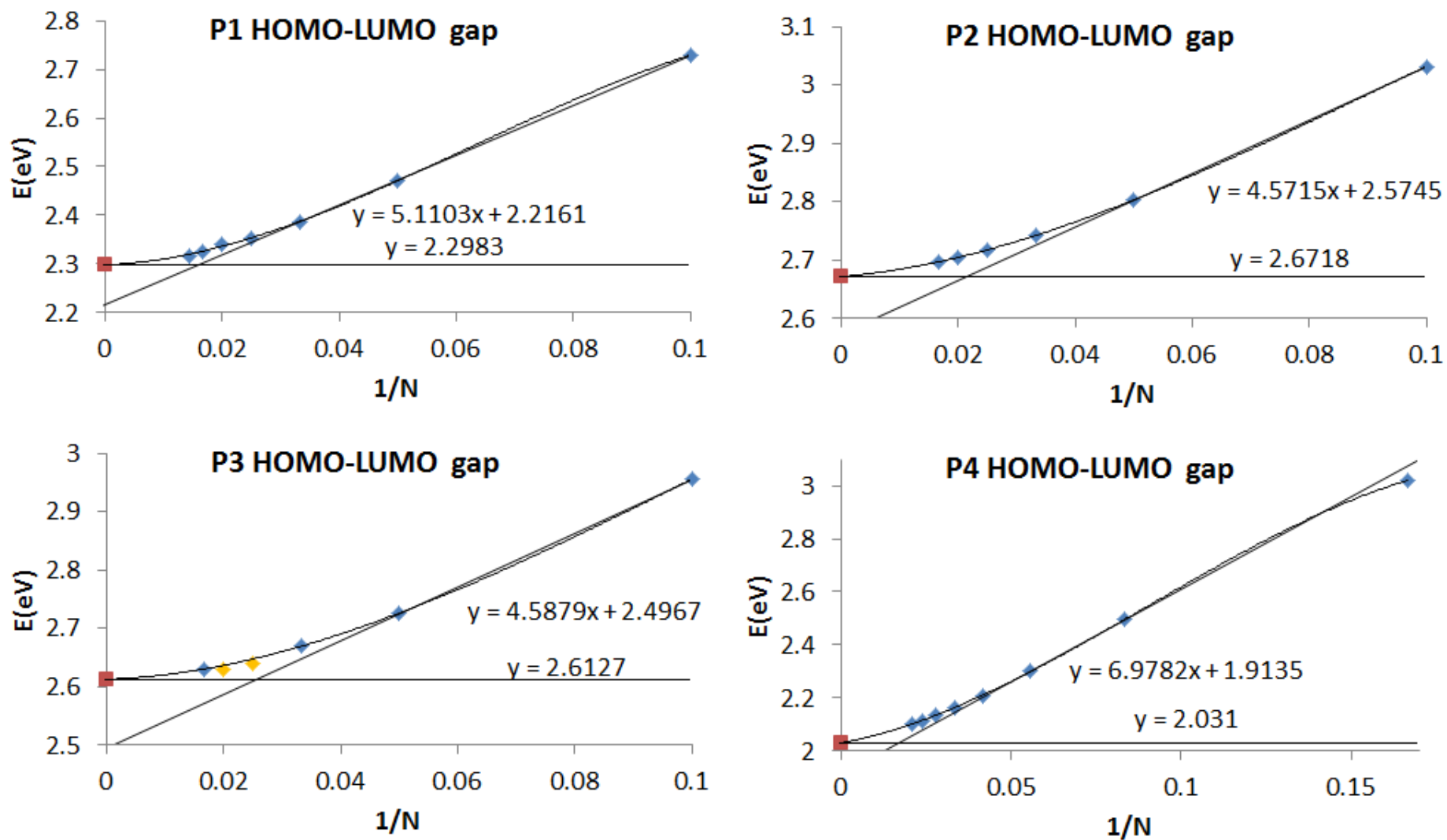


**Figure 11.** Determination of the  $N_{MCC}$  values of polymers P1–P4. The red squares denote the extrapolated HOMO-LUMO gaps at the infinite chain lengths. Yellow data points were not used in the extrapolation.

### Polymer – PCBM interaction

The exact HOMO and LUMO energy levels of the polymers P1 and P4, PC<sub>60</sub>BM, and PC<sub>70</sub>BM calculated for the isolated molecules and the combined polymer – PCBM pairs are presented in Table S5.

**Table S5.** Energy levels of P1, P4, PC<sub>60</sub>BM and PC<sub>70</sub>BM. Letters i) – iii) refer to positions of the PCBMs with respect to the polymers as discussed in the article.

	PC <sub>60</sub> BM HOMO	P1 HOMO	PC <sub>60</sub> BM LUMO	P1 LUMO	PC <sub>70</sub> BM HOMO	P1 HOMO	PC <sub>70</sub> BM LUMO	P1 LUMO
isolated	-5.566	-5.037	-3.003	-2.323	-5.518	-5.037	-2.980	-2.323
i)	-5.626	-5.022	-3.064	-2.315	-5.560	-5.022	-3.028	-2.311
ii)	-5.570	-4.992	-3.005	-2.273	-5.526	-4.992	-2.995	-2.269
iii)	-5.520	-4.948	-2.951	-2.237	-5.485	-4.964	-2.953	-2.249

	PC <sub>60</sub> BM HOMO	P4 HOMO	PC <sub>60</sub> BM LUMO	P4 LUMO	PC <sub>70</sub> BM HOMO	P4 HOMO	PC <sub>70</sub> BM LUMO	P4 LUMO
isolated	-5.566	-5.111	-3.003	-2.181	-5.518	-5.111	-2.980	-2.181
i)	-5.638	-5.064	-3.077	-2.137	-5.570	-5.089	-2.968	-2.156
ii)	-5.554	-5.047	-2.983	-2.125	-5.463	-5.182	-2.930	-2.192
iii)	-5.551	-5.105	-2.969	-2.242	-5.467	-5.237	-2.933	-2.230

### Combined polymer:PCBM film emission decay

The fluorescence emission decays were measured using 483 nm excitation and 710 nm monitoring wavelengths by TCSPC method.

**Table S6.** Fluorescence emission lifetimes and amplitudes of the polymer:PCBM active layers.

Sample	Mass ratio (mg)	$\tau_1$ (ns)	$A_1$	$\tau_2$ (ns)	$A_2$	$\tau_3$ (ns)	$A_3$	$\tau_4$ (ns)	$A_4$
P1:PC <sub>60</sub> BM	1.3 : 7.3	3.871	0.004	0.093	0.132	0.832	0.040	-	-
P1:PC <sub>70</sub> BM	1.0 : 4.3	3.867	0.001	0.106	0.231	0.625	0.263	-	-
P2:PC <sub>60</sub> BM	1.4 : 7.6	3.867	0.001	0.106	0.017	0.796	0.011	-	-
P3:PC <sub>60</sub> BM	1.7 : 7.1	3.867	0.0003	0.106	0.004	1.008	0.003	-	-
P4:PC <sub>60</sub> BM	1.7 : 4.4	0.971	0.021	0.530	-0.003	0.208	0.085	0.045	0.655
P4:PC <sub>70</sub> BM	1.6 : 4.8	0.798	0.012	0.561	0.039	0.122	0.079	0.0007	-0.041

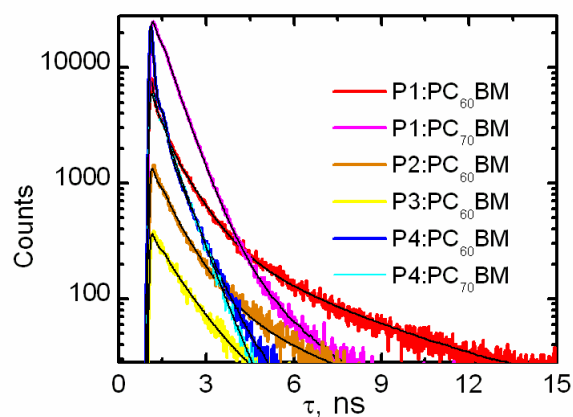


**Figure 12.** Emission decay curves and their fits (black lines) of the polymer:PCBM active layers.